

REDUCING THE PEAK TO AVERAGE POWER RATIO OF MIMO-OFDM SYSTEMS

Asim M. Mazin and Garth V. Crosby

College of Engineering, Southern Illinois University Carbondale

asimmazin@siu.edu, garth.crosby@siu.edu

ABSTRACT

In this paper, we proposed a particle swarm optimization (PSO) based partial transmit sequence (PTS) technique in order to achieve the lowest Peak-to-Average Power Ratio (PAPR) in Multiple Input Multiple Output- Orthogonal Frequency Division Multiplexing (MIMO-OFDM) systems. Our approach consist of applying the PSO based PTS on each antenna of the system in order to find the optimal phase factors, which is a straightforward method to get the minimum PAPR in such a system. The simulation results demonstrate that the PSO based PTS algorithm when applied to MIMO-OFDM systems with a wide range of phase factors, tends to give a high performance. In addition, there is no need to increase the number of particles of the PSO algorithm to enhance the performance of the system. As a result of this, the complexity of finding the minimum PAPR is kept at a reasonable level.

KEYWORDS

MIMO-OFDM, PTS, PSO, PAPR, CCDF.

1. INTRODUCTION

Sending high data rate over a wireless channel has been a challenge for researchers. Due to the wireless channel environment phenomenon called fading and the additive noise, transmitting high data rate is not a simple task to accomplish. One solution to this problem is by using a combination of multiple-input multiple-output (MIMO) with orthogonal frequency division multiplexing (OFDM). The resulting signal of this combination has multi-path delay tolerance and immunity to frequency selective channel fading. In addition, such a system benefits from the high bandwidth efficiency of the OFDM. These positive characteristics make MIMO- OFDM a promising candidate for high data rate wireless communications. However, high peak-to-average power ratio (PAPR) of the transmitted signal is a major drawback of the OFDM scheme. Since MIMO-OFDM system is based on OFDM, it also has the same issue [1]. This high PAPR is sensitive to nonlinear distortion, which is caused by the high power amplifier (HPA). The nonlinear distortion generates inter-symbol interference (ISI) and inter-modulation, which increases the bit error rate [2].

Many techniques have been proposed in the literature to effectively address the high PAPR in OFDM based systems. These approaches include the clipping techniques (that employ clipping or nonlinear saturation around the peaks to reduce PAPR), coding techniques, and probabilistic (scrambling) techniques.

In this paper, we study PAPR reduction in MIMO-OFDM using PTS. We apply a straightforward method, which is implemented by applying the PTS algorithm on each of the system's antennas. This technique is called Independent PTS (IPTS) [3]. In addition, we use the PSO algorithm to solve the phase optimization problem. Our primary contribution is a novel way of reducing the PAPR in MIMO-OFDM system by using the PSO algorithm.

The rest of this paper is organized as follows. In section II, the related works are presented. In section III we describe our system model. The simulation results of the PSO based PTS MIMO-OFDM algorithm are presented and discussed in section IV. We conclude the paper in section V.

2. RELATED WORKS

The PSO is a typical population-based random search algorithm developed by Eberhart and Kennedy in 1995. The algorithm has been widely used in various fields due to its effectiveness in performing difficult practical optimization problems. In addition, PSO obtains better results in faster, cheaper ways, and with fewer parameters to be adjusted compared to several other methods.

In CDMA communication a multiuser detector for DS-CDMA systems based on PSO algorithm was proposed. This resulted in a near optimal performance [4]. The PSO algorithm was used in electromagnetic to design CPW-fed planar monopole antenna with an optimal multiband operation, which is suitable for use in the personal communication systems and 2.4/5.2 GHz wireless local-area network (WLAN) applications. The design process used the PSO to optimize the performance of the antenna by choosing the most appropriate configuration parameters of the CPW-fed antenna [5].

The PTS technique is used to solve optimization problem, which is required when finding the optimal phase factors that achieve low PAPR. The complexity of the PTS algorithm is a trade-off for its performance. Dealing with the complexity issue of PTS, a novel PTS technique based on gradient descent search, which is useful in solving combinatorial optimization problems, was proposed in [6]. The objective of the technique is to find the phase factors that achieve PAPR statistics close to that of the ordinary PTS technique with reduced search complexity and little performance degradation. In the PTS technique, it is necessary to send bits of side information to the receiver side. A PTS with a coded side information technique is proposed in [7]. This approach utilized a code table in the transmitter and the receiver. The code side information table contains a codeword for each phase factor candidate.

The PSO-PTS is a scrambling technique that was proposed in the literature to reduce the PAPR in OFDM systems [8], [9]. Both research works solved the phase factors optimization problem by using PSO, which is an evolutionary method used to determine an optimum solution for any optimization problem such as PTS. Hung *et al.* [9] enhanced the performance of PSO based PTS by increasing the number of particles (Generations) when the phase weight factor was chosen from a small set. However, the relationship between the number of particles and the reduction of PAPR was not clearly investigated. In this paper we present a PSO based PTS reduction technique for MIMO-OFDM and demonstrate the performance of PSO when the phase factors set is large. To best of our knowledge, this has never been done.

3. OFDM-MIMO SYSTEMS

In this section we introduce the theoretical foundations for our research work. We present an introduction to Orthogonal Frequency Division Multiplexing (OFDM) by introducing the multicarrier modulation and compare and contrast it with single carrier modulation. Then, we describe the modulation and the demodulation process of OFDM systems and introduce the concept of multiple-input-multiple output (MIMO) systems.

Multicarrier (MC) modulation is currently used in many modern wireless systems. However, it has been around since the late 1950's. In 1971, Weinstein and Ebert [10] proposed time-limited MC transmission by using the discrete Fourier transform (DFT), which is what we call OFDM today. In 1995 the European Telecommunications Standards Institute Digital Audio Broadcasting (ETSI DAB) introduced the first OFDM-based wireless for digital audio broadcasting. During the period 1997 to 2005 many OFDM-based systems were introduced, such as terrestrial digital video broadcasting, wireless LAN IEEE 802.11a, broadband wireless MAN IEEE 802.16a/d, and OFDM-based mobile cellular networks [11].

3.1. Single Carrier Modulation

In single carrier modulation system the transmit symbols, a_{nT} , each has a period of T seconds, that is, a data rate of $R = 1/T$. This data is pulse-shaped by the transmit filter $g_T(t)$ at the transmitter, then it passes through a band-limited channel $h(t)$ with a bandwidth W . Upon receiving the transmitted symbols through the noisy channel they are processed by the filter, equalizer, and detector at the receiver side. This process is illustrated in Figure 1. The output of the system can be expressed as

$$y(t) = \sum_{n=-\infty}^{\infty} a_{nT} g(t - nT) + z(t) \quad (1)$$

where $z(t)$ is additive noise and $g(t)$ is the overall impulse response of the system and can be expressed as

$$g(t) = g_T(t) * h(t) * g_R(t) * h^{-1}(t) \quad (2)$$

where $[*]$ is the convolution process, $g_T(t)$ is the response of the transmit filter, $h(t)$ is the channel response, $g_R(t)$ is the response of the receive filter, and $h^{-1}(t)$ is the response of the equalizer.

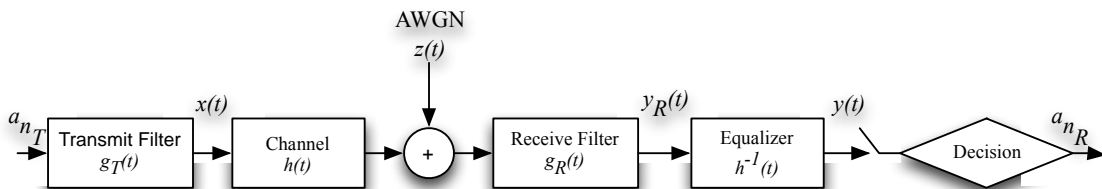


Figure 1. Single carrier baseband communication system scheme (taken from [12])

In order to support a higher data rate, the single-carrier transmission system requires wider bandwidth. For symbol rate R_s the minimum required bandwidth is the Nyquist bandwidth, which is given by $R_s/2$ Hz. However, as the symbol rate increases, the signal bandwidth becomes larger. When the signal bandwidth becomes larger than the coherence bandwidth of the wireless channel, the link suffers from multi-path fading, which introduces inter-symbol interference (ISI). To deal with the ISI in single carrier system an expensive adaptive equalizer needs to be employed. As a result, a high data rate over a single carrier system may not be a practical solution due to the complexity of the equalizer in the receiver [12].

3.2. Multicarrier Modulation

Due to the limitation of single carrier modulation as we have mentioned, multiple carrier systems are instead utilized to support high data rate. All MC modulation techniques are based on the concept of *channel partitioning*. Channel partitioning methods divide a wideband, spectrally shaped transmission channel into a set of parallel narrowband sub-channels. The channel partitioning can be established for both the continuous-time case and discrete-time case. We will focus on the discrete-time case since it is a more practical technique. and the OFDM, which is a discrete-time case of MC modulation [13].

A basic multicarrier transmitter and receiver are illustrated in Figure 2 and Figure 3 respectively. The simple idea of MC is to convert a high data rate signal of R bps and a passband bandwidth of B into L parallel sub-streams, each with data rate R/L and passband bandwidth B/L . As long as the number of subcarriers is sufficiently large to ensure that $R/L \ll B_c$, where B_c is the coherence bandwidth of the channel, it can be guaranteed that each subcarrier will experience approximately flat fading [14].

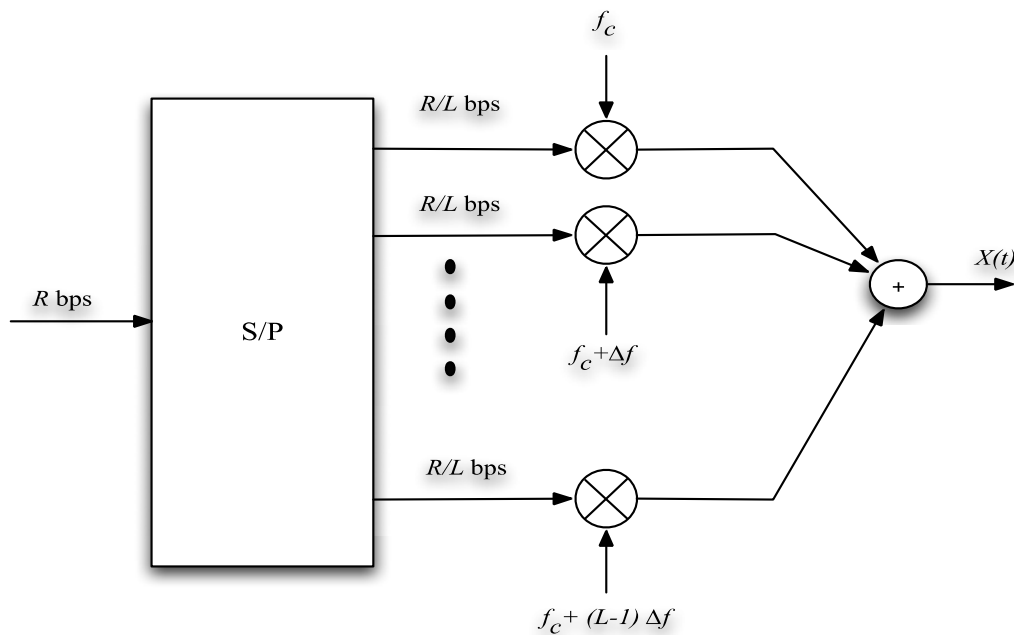


Figure 2. A basic multicarrier transmitter (taken from [14])

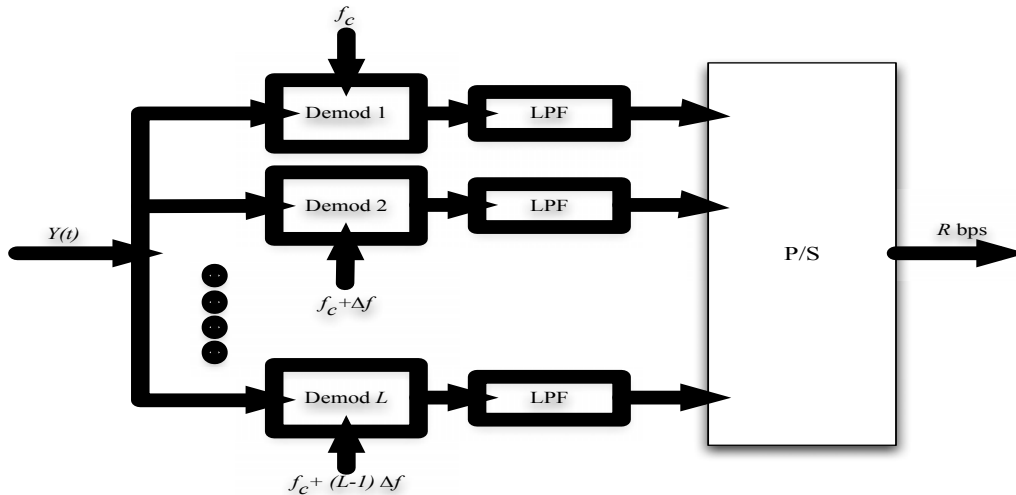


Figure 3. A basic multicarrier receiver (taken from [14])

3.3. Advantages and disadvantages of OFDM

OFDM has several advantages that make it the best candidate for the next generation of wireless networks. These include:

- A low-complexity modulation that can be implemented using FFT/IFFT algorithm.
- High spectral efficiency.
- Robustness against ISI and multipath fading.

Notwithstanding, there are a few significant limitations. These are as follows:

The major disadvantage of OFDM is the high Peak-Average Power Ratio. We focus on this

- particular problem and propose a solution in this paper.
- OFDM is vulnerable to frequency and time offsets

3.4. MIMO System Model

As was previously mentioned the demand for capacity in wireless communication has been rapidly increasing worldwide. On the other hand the radio spectrum is limited and cannot meet this demand with legacy communication systems. Multi-input Multi-output antenna, which was first introduced by Teltar and Foschini, is one of the most significant solutions for this capacity issue [15].

A MIMO system can be achieved with multi-element array. Figure 4 illustrates a MIMO system with a transmit array of M_T antennas and a receive array of M_R antennas. The transmitted matrix is a $M_T \times 1$ column matrix \mathbf{x} where x_i is the i th component, transmitted from antenna i . The channel is assumed to be a Gaussian channel such that the elements of \mathbf{x} are considered to be independent identically distributed (i.i.d) Gaussian variables. Also, we assume that the signals transmitted from

each antenna have equal E_x/M_T . The covariance matrix of this transmitted signal is given by

$$R_{xx} = \frac{E_x}{M_T} I_{M_T} \quad (3)$$

where E_x is the power across the transmitter irrespective of the number of antennas M_T and I_{M_T} is an $M_T \times M_T$ identity matrix. The channel matrix \mathbf{H} is a $M_R \times M_T$ complex matrix. The component $h_{i,j}$ of the matrix is the fading coefficient from the j th transmit antenna to the i th receive antenna. We ignore signal attenuation and antenna gains. Thus, the normalization constraint for the elements of \mathbf{H} , for deterministic channel is given by

$$\sum_{j=1}^{M_T} |h_{i,j}|^2 = M_T, i = 1, 2, \dots, M_R \quad (4)$$

for the random elements channel. The normalization is applied to the expected value of (4). The noise \mathbf{n} at the receiver is another column matrix of size $M_R \times 1$, the components of \mathbf{n} are zero mean circularly symmetrical complex Gaussian (ZMCSCG) variables. The covariance matrix of the noise is

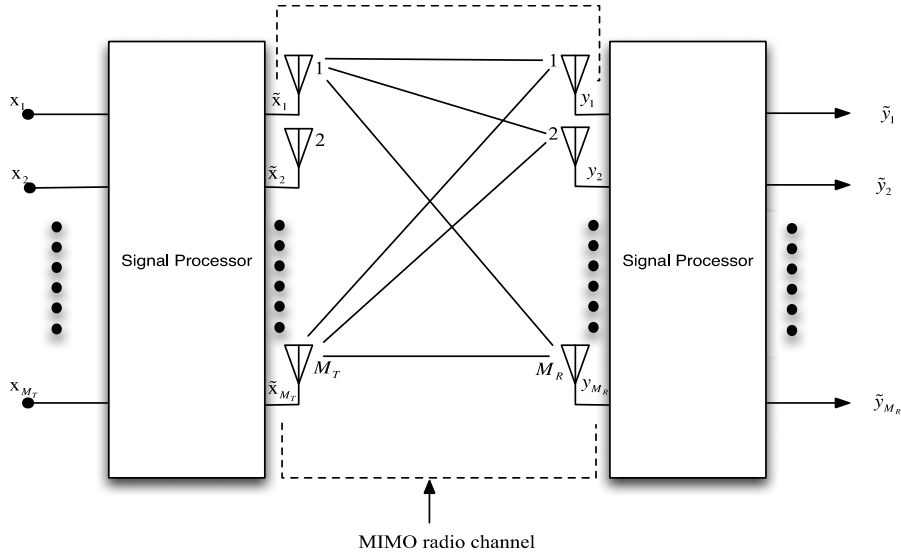


Figure 4. Block diagram of a MIMO system

$$R_{nn} = E\{nn^H\} \quad (5)$$

Therefore, the received vector can be expressed as

$$\mathbf{r} = \mathbf{H}\mathbf{x} + \mathbf{n} \quad (6)$$

The received signal covariance matrix is defined as $E\{\mathbf{r}\mathbf{r}^H\}$ of (6)

$$R_{rr} = \mathbf{H}R_{xx}\mathbf{H}^H \quad (7)$$

while the total signal power can be expressed as $\text{tr}\{R_{rr}\}$.

3.4.1. MIMO System Capacity

The capacity of the MIMO system is defined as the maximum possible transmission rate such that the probability of error is arbitrarily small. We assume that the channel knowledge is unavailable at the transmitter and known only at the receiver. The capacity of MIMO channel is defined as

$$C = \max_{f(x)} I(x;y) \quad (8)$$

where $f(x)$ is the probability distribution of the vector x and $I(x;y)$ is the mutual information between vectors x and y . Thus we can write

$$I(x;y) = H(y) - H(y | x) \quad (9)$$

where $H(y)$ is the differential entropy of the vector y , while $H(y | x)$ is the conditional differential entropy of the vector y , given the knowledge of the vector x . Since the vectors x and n are independent, $H(y | x) = H(n)$. Thus Equation (9) can be rewritten as

$$I(x;y) = H(y) - H(n) \quad (10)$$

the (10) can be maximized $I(x;y)$ by maximizing $H(y)$. The covariance matrix of y , $R_{yy} = \{yy^H\}$, satisfies

$$R_{yy} = \frac{E_x}{M_T} H R_{xx} H^H + N_0 I_{M_R} \quad (11)$$

where $R_{xx} = \{xx^H\}$ is the covariance matrix of x . It has been proven that the differential entropy $H(y)$ is maximized when y is (ZMCSCG), that implies x must also be a (ZMCSCG) vector. The differential entropies of the vectors y and n are given by

$$H(y) = \log_2 \left(\det(\pi e R_{yy}) \right) \text{ bps/Hz} \quad (12)$$

$$\text{and} \quad (13)$$

$$H(n) = \log_2 \left(\det(\pi e \sigma^2 I_{M_R}) \right) \text{ bps/Hz}$$

Therefore, $I(x;y)$ in (8) can be reduced to

$$I(x;y) = \log_2 \det \left(I_{M_R} + \frac{E_x}{M_T N_0} H R_{xx} H^H \right) \text{ bps/Hz} \quad (14)$$

and from (9), the capacity of the MIMO channel is given by

$$C = \max_{\text{Tr}(R_{xx})=M_T} \log_2 \det \left(I_{M_R} + \frac{E_x}{M_T N_0} H R_{xx} H^H \right) \text{ bps/Hz} \quad (15)$$

The capacity C in (15) is called the error-free spectral efficiency and can be sustained reliably over the MIMO link.

3.4.2. MIMO Space-Time Code

Space-Time Code is a powerful scheme that combines coding with transmit diversity to achieve high diversity performance in wireless systems. In this work, we present the Alamouti code encoder. The Alamouti code encoder is illustrated in Figure 5 where the information bits are first modulated using an M -ary modulation scheme. The encoder then takes a block of two modulated symbols X_1 and X_2 in each encoding operation and passes it to the transmit antennas according to the code matrix,

$$X = \begin{pmatrix} X_1 & -X_2^* \\ X_2 & X_1^* \end{pmatrix} \quad (16)$$

The first and second column of (16) represent the first and second transmission period, respectively. The first row corresponds to the symbols transmitted from the first antenna and the second row corresponds to the symbols transmitted from the second antenna. Furthermore, during the first and second symbol periods both the first and second antenna transmits. This implies that the transmission process occurs both in space (across two antennas) and time (two transmission periods).

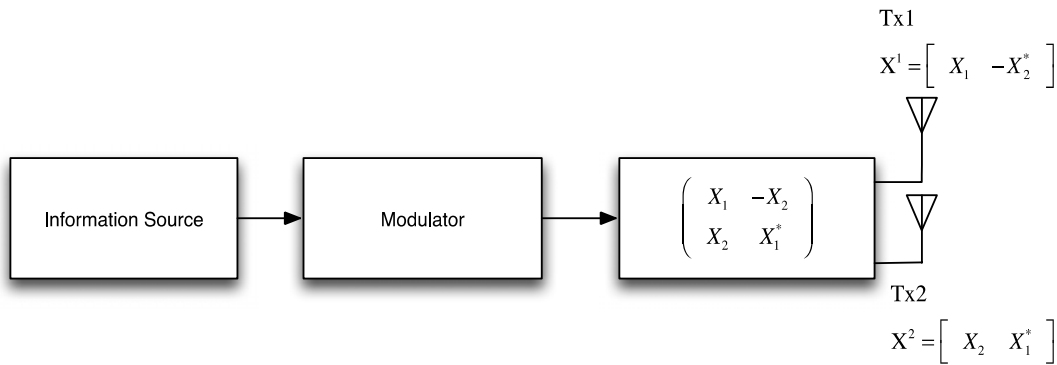


Figure 5. Block diagram of the Alamouti space-time encoder.

3.4.3. MIMO-OFDM Structure

OFDM modulation can be used to transform the frequency-selective channel into a set of parallel frequency flat sub-channels, providing high spectrum efficiency and greatly eliminating ISI. In addition, a multicarrier system can be efficiently implemented in discrete time using an IFFT to act as a modulator and an FFT to act as a demodulator, so it is not very complex. Because OFDM allows sub-carriers frequency spectrum to partially overlap it has high spectrum efficiency and is considered to be an efficient modulation technique [16]. In practice, most wireless channels experiences frequency-selective fading, which makes the implementation of space-time coding very complicated. However, OFDM can transform the frequency-selective channel into a set of parallel frequency flat sub-channels that can reduce the complexity of space-time coding. The MIMO-OFDM system makes full use of its own characteristics to further enhance the system's total performance [17].

The transmitter and receiver blocks with 2 antennas both at the transmitter and the receiver of the MIMO-OFDM system is shown in Figure 6. At the transmitter, the source bit streams are mapped, passed via the Space-Time Code encoder and then mapped to their corresponding symbols with two outputs. Each symbol passes through a serial to parallel (S/P) converter and

becomes parallel data. Afterwards, the IFFT is performed, employing OFDM modulation in each sub-carrier. Time domain symbols are parallel to serial (P/S) converted and then a cyclic prefix (CP) is added in order to mitigate or eliminate ISI and ICI (inter-carrier interference). Lastly, the amplified modulated signals are transmitted.

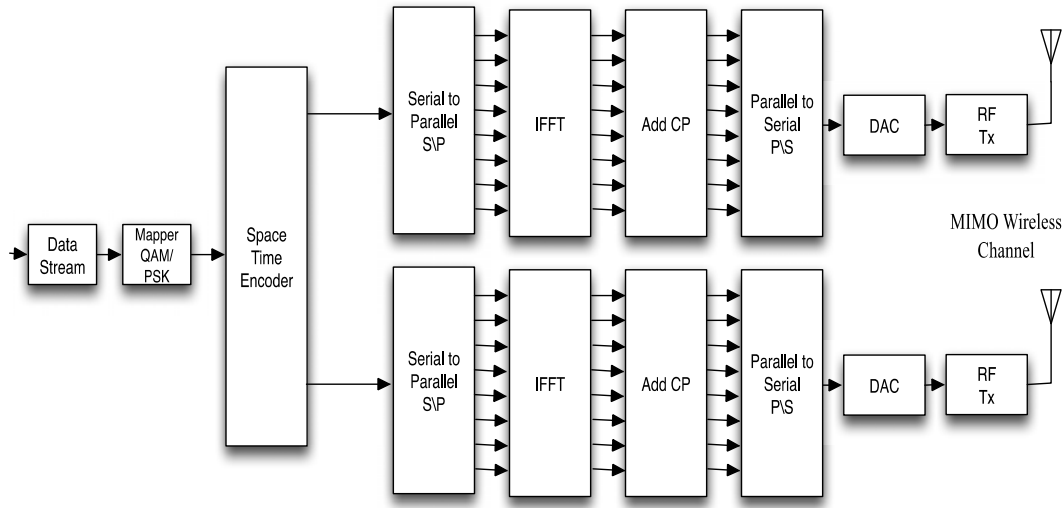


Figure 6. Block diagram of 2 antennas MIMO- OFDM transmittersystem

4. Peak to Average Power Ratio (PAPR)

The instantaneous output signal of an OFDM system often has large fluctuations compared to traditional single-carrier systems due to the sum of many narrowband signals in the time domain. This requires that system devices, such as power amplifiers, A/D converters and D/A converters, must have large linear dynamic ranges. If this is not satisfied, a series of undesirable interference is encountered when the peak signal goes into the non-linear region of devices at the transmitter, such as high out of band radiation and inter-modulation distortion. PAPR reduction techniques are therefore of great importance for OFDM systems [18].

4.1 The PAPR Problem

In general, even linear amplifier or DAC and ADC introduce a nonlinear distortion on their outputs due to their saturation characteristics caused by the input being much larger than its normal value. Figure 7 illustrates the characteristic of a high power amplifier (HPA), which is a typical AM/AM response for HPA. A high peak signal generates out-of-band energy and in-band distortion. These degradations may affect system performance. To avoid such nonlinear effects, a waveform with high peak power must be transmitted in the linear region of the HPA by decreasing the average power of the input signal. This is called (input) backoff (IBO) and results in a proportional output backoff (OBO). [12]

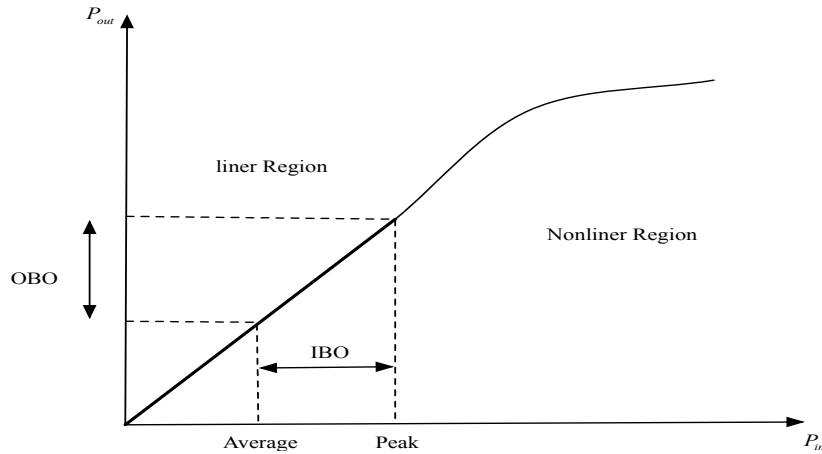


Figure 7. Input-output characteristic of a typical amplifier

The input backoff can be written as

$$IBO = 10 \log_{10} \frac{P_{inSat}}{\bar{P}_{in}} \quad (17)$$

where P_{inSat} is the saturation power, above which is the nonlinear region, and \bar{P}_{in} is the average input power. The amount of backoff is usually greater than or equal to the PAPR of the signal.

4.2 Quantifying the PAPR

As mentioned previously, the OFDM system transmit data over N parallel-frequency channels, the resulting waveform is the superposition of N narrowband signals. These N narrowbands are the result of N Point IFFT operations involving the sum of N complex numbers. According to the Central Limit Theorem, the output can be accurately modelled as complex Gaussian random variables with zero mean and variance $\sigma^2 = \frac{\epsilon_x}{2}$. The amplitude of the output signal can be expressed as

$$x[n] = \sqrt{(Re\{x[n]\})^2 + (Im\{x[n]\})^2} \quad (18)$$

which is Rayleigh distributed with parameter σ^2 . The output power can therefore be expressed as

$$x[n] = (Re\{x[n]\})^2 + (Im\{x[n]\})^2 \quad (19)$$

which is exponentially distributed with mean $2\sigma^2$. The PAPR of the transmitted OFDM signal can be defined as

$$PAPR = \frac{\max |x[n]|^2}{E[|x[n]|^2]}, \quad 0 \leq n \leq N - 1 \quad (20)$$

where $E[]$ denotes the expected value.

4.3 Probability Distribution Function of PAPR

The statistical description of the PAPR is the most commonly used due to the seldom occurrence of the maximum PAPR. The complementary cumulative distribution function (CCDF) can be expressed as

$$\text{CCDF} = 1 - \text{CDF} \quad (21)$$

As was mentioned previously, the output signal has an exponential distribution, thus

$$\text{CDF} = 1 - e^{-z} \quad (22)$$

and

$$\text{CCDF} = P(\text{PAPR} < Z) = (1 - (1 - e^{-z}))^N \quad (23)$$

Since the MIMO-OFDM systems are based on OFDM, they also suffer from the high PAPR issue. In this work, we use the CCDF as a metric to assess the performance of the proposed algorithm.

5.SYSTEM MODEL

In OFDM systems, the transmitted signal is the sum of orthogonal sub-carriers that are modulated by complex data symbols. For an OFDM system with N sub-carriers, the complex baseband signal can be written as

$$x(t) = \frac{1}{\sqrt{N}} \sum_{i=0}^{N-1} X_i e^{j2\pi i \Delta f t}, \quad 0 \leq t \leq T \quad (24)$$

where X_i is the complex data symbol at i -th sub-carrier, T is the duration of the OFDM symbol, and $\Delta f = 1/NT$ is the sub-carrier frequency spacing.

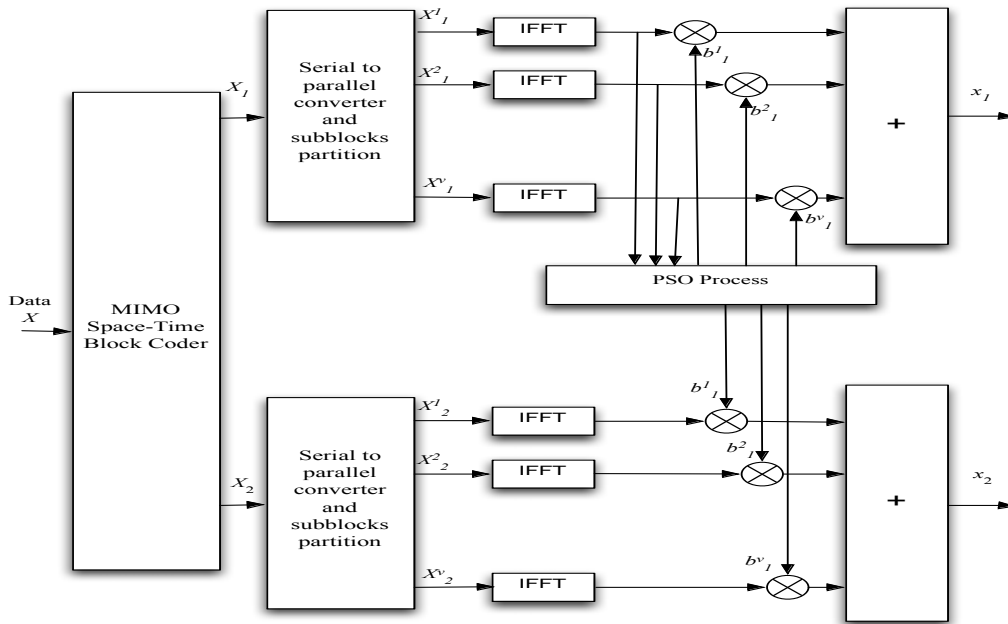


Figure 8. Block diagram of PTS based PSO scheme of MIMO-OFDM

5.1. PAPR definition in OFDM

By sampling $x(t)$ in time with time instance $t = (T/i)n$, the complex discrete baseband representation of an OFDM transmitted signal which is the output of IFFT operation in Figure 1 can be represented as

$$x(n) = \frac{1}{\sqrt{N}} \sum_{i=0}^{N-1} X_i e^{j2\pi ni/N}, \quad 0 \leq n \leq N - 1 \quad (25)$$

The PAPR of the transmitted OFDM signal in (24) can be calculated by equations (20) and (23).

5.2. PAPR definition in MIMO-OFDM

In MIMO-OFDM system the analysis of the PAPR performance is similar to the OFDM system with single antenna. The PAPR of the entire system is defined as the maximum of the PAPRs among all the transmit antennas [19].

$$\text{PAPR}_{\text{MIMO-OFDM}} = \max_{1 \leq i \leq m} \text{PAPR}_m \quad (26)$$

where m is the number of the transmitter antenna in the system, in this paper we assumed $m = 2$.

5.3. PTS in MIMO-OFDM

The PTS based PSO scheme of MIMO-OFDM system is illustrated in Figure 8. We employed Alamouti Space-Time Code as a MIMO encoder as in (16).

where \mathbf{X} is the modulated data signal. The PTS technique partitions each input complex data block ($\mathbf{X}_1, \mathbf{X}_2$) of N symbols into K disjoint sub-blocks as

$$X_1 = [X_1^1, X_1^2, \dots, X_1^K] \quad (27)$$

$$X_2 = [X_2^1, X_2^2, \dots, X_2^K] \quad (28)$$

Then each partitioned sub-block of each antenna is multiplied by a corresponding complex phase factor $b^k = e^{j\varphi_k}, k = 1, 2, \dots, K$, subsequently taking its IFFT to yield

$$\mathbf{x} = \text{IFFT} \left\{ \sum_{k=1}^K (b\mathbf{X})^k \right\} = \sum_{v=1}^V (b\mathbf{x})^k \quad (29)$$

where \mathbf{x}^k is represented a partial transmit sequence (PTS). The phase factor vector is chosen based on a PSO algorithm that minimize PAPR as

$$\mathbf{b} = \arg \min_b \left\{ \max \left| \sum_{k=1}^K (b\mathbf{x})^k \right| \right\} \quad (30)$$

where b is given by $b^k = e^{j\varphi_k}$ and $\varphi_k \in \{0, 2\pi\}$. To reduce the complexity of the system, the PSO algorithm is employed on the data stream of antenna 1 to get the optimal phase factors that ensure the lowest PAPR. The phase factors obtained are re-used on the data stream on antenna 2.

We assumed that the bit side information is coded into unique codeword and is sent, along with the data, to the receiver side to be decoded in order to extract the information [7].

5.4. Particle Swarm Optimization Based PTS

We used the PSO as an optimizer to solve the phase factor problem in (32), which is shown as PSO process block in Figure 1. In the PSO algorithm the possible solution space of the problem is called particles, which is φ_k in the PTS based PSO scheme. By moving the particles around in the search-space, the optimal solution of the phase problem will be reached. During the movement of the particles, each particle is characterized by two parameters: position and velocity. The PSO algorithm evaluates the particles with the fitness value, which is PAPR in (20), the objective function. A solution space is randomly generated, which is a matrix of size $S \times K$, where S is the number of particles and K is the number of disjoint sub-block. In other words, the solution space is a matrix its rows are $[\varphi_1, \varphi_2, \dots, \varphi_k]$. Since the PSO is an iterative algorithm, in the t^{th} iteration each particle can be described by its position vector $Y_{sk}^t = (y_{s1}^t, y_{s2}^t, y_{s3}^t, \dots, y_{sK}^t)$ and velocity vector $V_{sk}^t = (v_{s1}^t, v_{s2}^t, v_{s3}^t, \dots, v_{sK}^t)$, where $s \in [1, S]$ and $Y_{sk}^t \in R$ and R denotes the domain of the objective function. The PSO algorithm searches the solution space for the optimum

solution by using iteration process. In every iteration each particle updates itself by tracking two best positions. These are called the local best position, which is the best solution this particle has achieved $p_{sk} = (p_{s1}, p_{s2}, p_{s3}, \dots, p_{sK})$, and the global best position $p_{sk}^g = (p_{s1}^g, p_{s2}^g, p_{s3}^g, \dots, p_{sK}^g)$ which is the best position obtained so far by any particle in the whole swarm. The updating process of the position and velocity of each particle can be expressed as

$$\mathbf{V}_{sk}^{t+1} = w\mathbf{V}_{sk}^t + c_1r_1(p_{sk}^t - Y_{sk}^t) + c_2r_2((p_{sk}^t)^g - Y_{sk}^t) \quad (31)$$

$$\mathbf{Y}_{sk}^{t+1} = \mathbf{Y}_{sk}^t + \mathbf{V}_{sk}^t \quad (32)$$

where c_1 and c_2 are the acceleration terms. The constant r_1 and r_2 are uniform distribution random number in the range of [0,1]; w is the inertia factor. The PSO algorithm was employed over antenna 1 as shown in Figure 8. The above discussion of the PSO-PTS can be summarized by the flowchart in Figure 9.

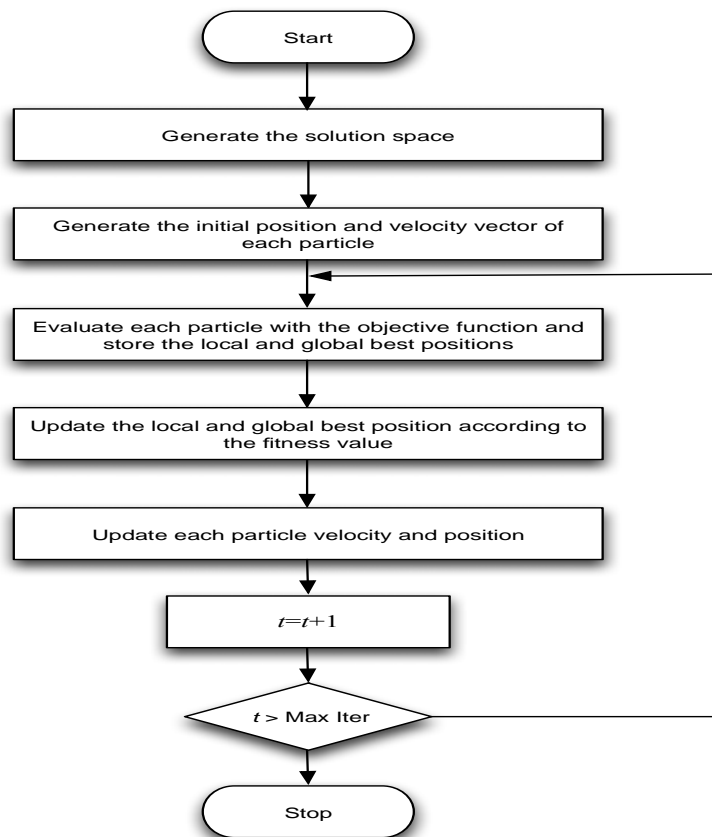


Figure 9. PSO-PTS algorithm flowchart

6. SIMULATION RESULTS AND DISCUSSION

We used MATLAB simulation to evaluate the performance of our PSO-PTS algorithm on MIMO-OFDM systems. We focused on the effect of our algorithm on the PAPR. The simulation had two antennas at the transmitter side as shown in Figure 1. We used a 16 QAM modulation scheme with $N = 256$ carriers. The phase weighted factors, $\varphi_k \in [0, 2\pi]$, were randomly generated.

The Complementary Cumulative Distribution Function (CCDF) of PAPR was calculated by generating 2000 random OFDM frames. The constant acceleration $c_1 = c_2 = 2$ and the inertia factor w was calculated by using

$$w = (w_{max} - w_{min}) \times \frac{Itr_{max} - Itr_{min}}{Itr_{max}} + w_{min} \quad (33)$$

where Itr_{max} and $Itr_{current}$ are the maximum iteration and the current iteration respectively. $w_{max} = 0.9$ and $w_{min} = 0.4$. It can be noted from equation (33) that w decreased linearly from 0.9 to 0.4 during the simulation period.

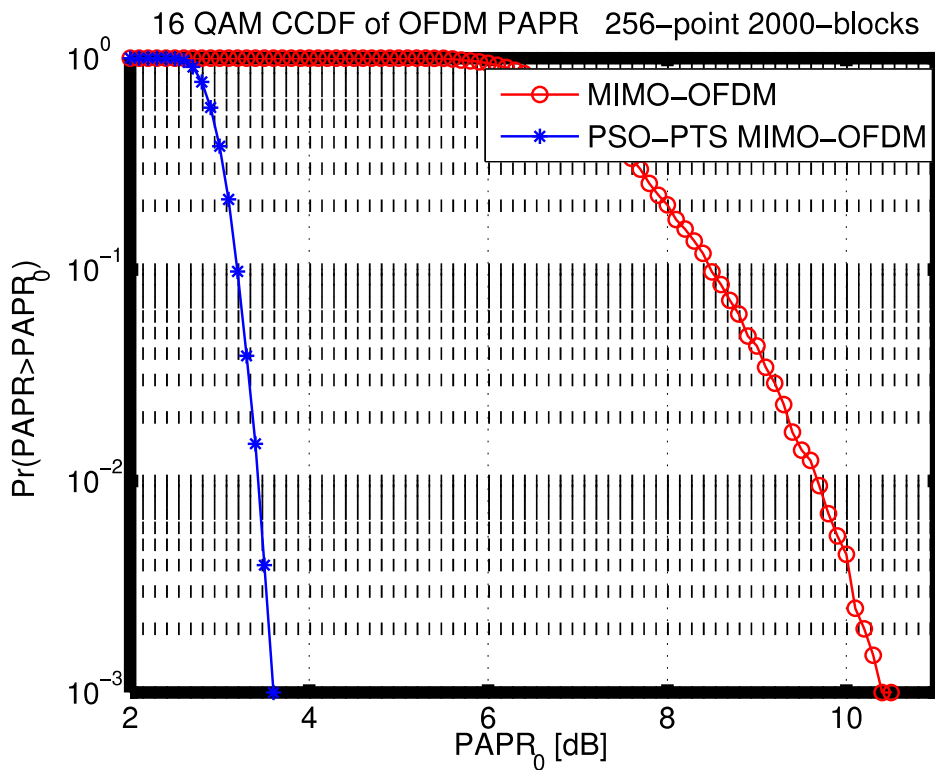


Figure 10. CCDF of the PAPR of MIMO-OFDM using PSO-PTS and CCDF of the original MIMO-OFDM

In Figure 10 the CCDF of PAPR of the PSO-PTS MIMO-OFDM (with 16 sub-blocks, 256 carriers, and 10 particles) is compared with the original PAPR MIMO-OFDM. The probability that the PAPR of PSO-PTS MIMO-OFDM signal exceeds 3.6 dB was 0.0025 while with the same probability; the PAPR of the original MIMO-OFDM system exceeds 10.1 dB.

Figure 11 illustrates the OFDM symbol in the time domain through antenna 1 before and after the PSO-PTS algorithm. It is obvious from the graph that the backoff margin is very small in case of using PSO-PTS in comparison with the case without using it. As a result, the transmitted waveform will be transmitted in the linear region of HAP.

For simplicity, we used adjacent portioning technique. By increasing the number of sub-blocks of the PSO-PTS MIMO-OFDM system, the performance of the system was enhanced. The CCDF of

PAPR of the PSO-PTS MIMO- OFDM when $K = \{4, 8, 16\}$ is shown in Figure 12. The probability that PAPR exceeds 3.4 dB is 0.0125 when $K = 16$; the probability that the PAPR exceeds 3.8 dB was 0.0105 when $K = 8$, and PAPR exceeds 4.4 dB was 0.01 when $K = 4$. Figure 13 illustrates the performance of PSO-PTS when different constants accelerations are used. The probability that the PAPR exceeds 3.4 dB is 0.01 when $c_1 = c_2 = 2$ and exceeds 3.435 dB is 0.0099 when $c_1 = c_2 = 0.3$. It can be noted from the graph that $c_1 = c_2 = 2$ has slightly better performance than other combinations.

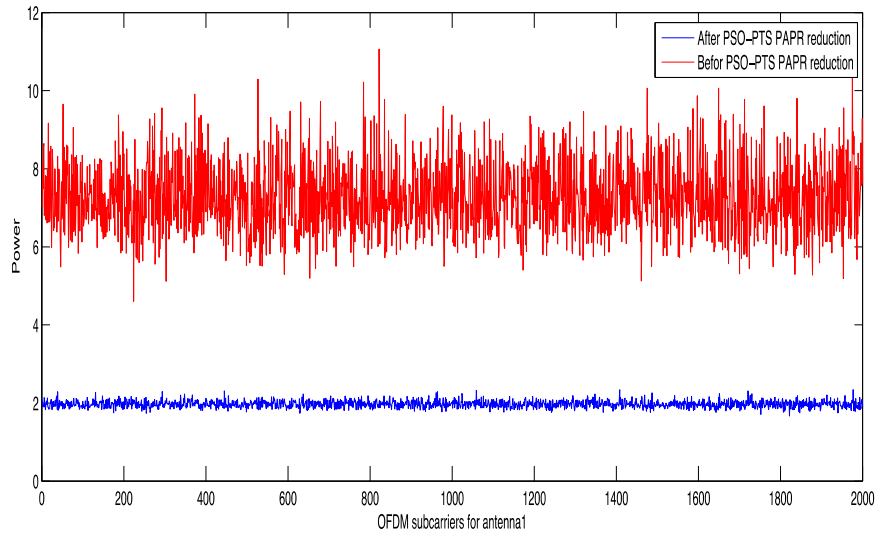


Figure 11. comparison between the time domain OFDM symbol through

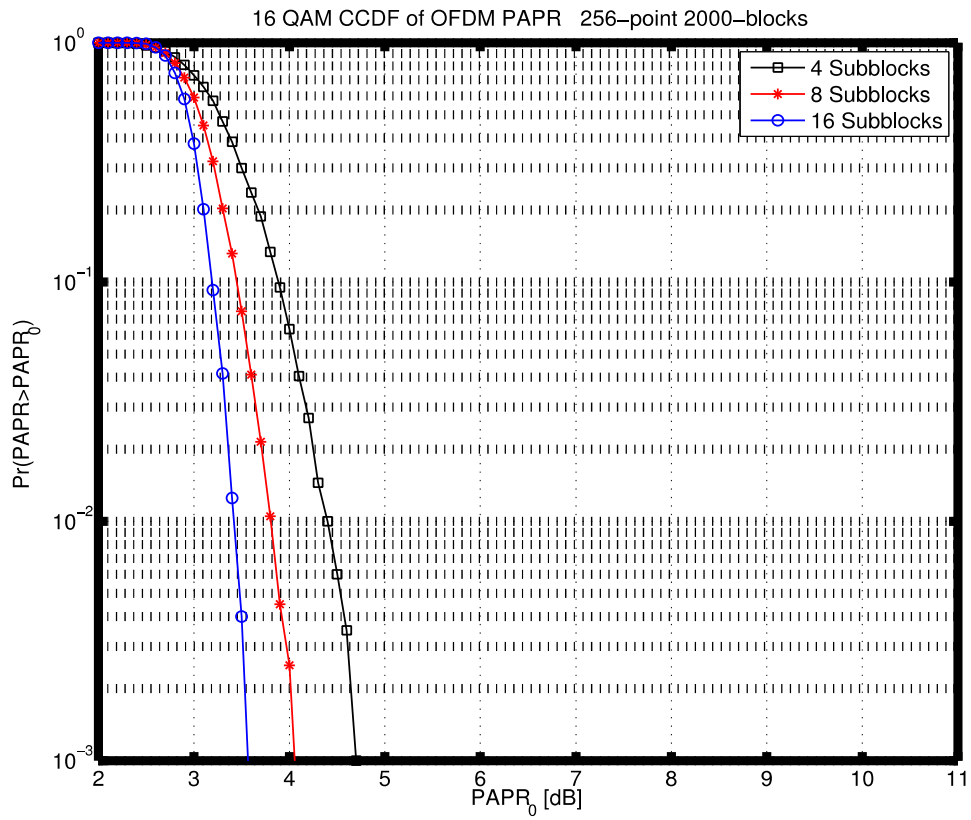


Figure 12. CCDF of the PAPR of MIMO-OFDM using PSO-PTS for different number of sub-blocks

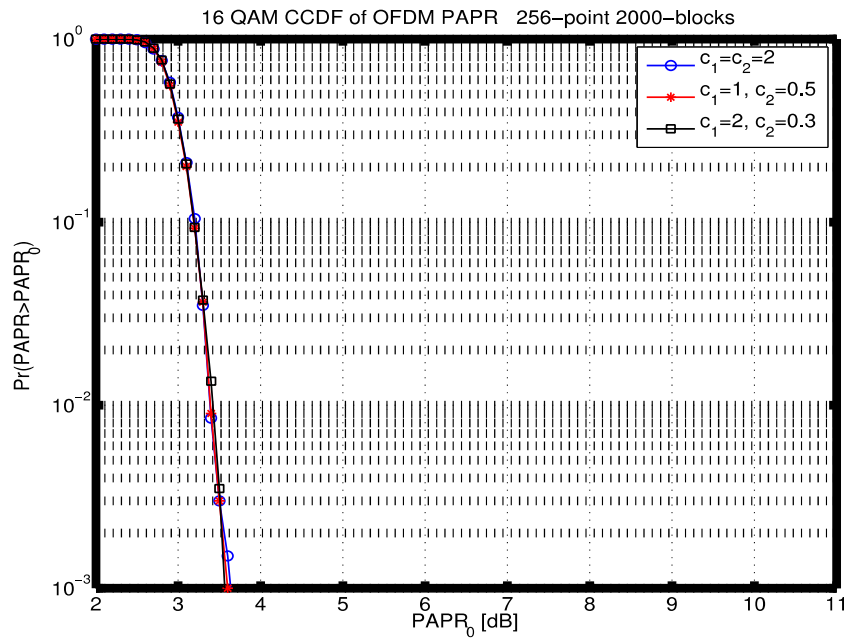


Figure 13. CCDF of the PAPR of MIMO-OFDM using PSO-PTS for different combination of acceleration constants

7. CONCLUSION

In this paper, the PAPR of MIMO-OFDM systems using PSO algorithm was studied. The performance of the system was evaluated by calculating the CCDF. Applying the PSO-PTS algorithm on MIMO-OFDM resulted in 6.5 dB gains in comparison to the original MIMO-OFDM system. By choosing the phase factors with high degrees of freedom the number of needed particles was low and the performance of the PSO algorithm was enhanced. The complexity of the search was low since the number of particles was also kept low. The system modeled had 2 antennas at the transmitter. The effects on the PAPR by increasing the number of antennas and applying the PSO-PTS in different ways to keep the complexity of the system reasonable are worthy of investigation.

REFERENCES

- [1] S. H. Han and J. H. Lee, "An overview of peak-to-average power ratio reduction techniques for multicarrier transmission," *IEEE Wireless Communications*, vol. 12, pp. 56 – 65, April 2005.
- [2] O.-J. Kwon and Y.-H. Ha, "Multi-carrier pap reduction method using sub-optimal PTS with threshold," *IEEE Transactions on Broadcasting*, vol. 49, pp. 232 – 236, June 2003.
- [3] X. Yan, W. Chunli, and W. Qi, "Research of peak-to-average power ratio reduction improved algorithm for MIMO-OFDM system," in the proceedings of WRI World Congress on Computer Science and Information Engineering, vol. 1, pp. 171 –175, April 2009.
- [4] H. -L. Hung, Y. -F. Huang, and J. -H. Wen, "A particle swarm optimization based multiuser detector for DS-CDMA communication systems," in the proceedings of IEEE International Conference on Systems, Man and Cybernetics (SMC), vol. 3, pp. 1956 –1961, Oct. 2006.

- [5] W. -C. Liu, "Design of a multiband CPW-FED monopole antenna using a particle swarm optimization approach," in IEEE Transactions on Antennas and Propagation, vol. 53, pp. 3273 – 3279, Oct. 2005.
- [6] S. H. Han and J. H. Lee, "PAPR reduction of OFDM signals using a reduced complexity PTS technique," Signal Processing Letters, IEEE, vol. 11, pp. 887 – 890, Nov. 2004.
- [7] C. Pradabpet, S. Yoshizawa, S. Chivapreecha, and K. Dejhan, "New PTS method with coded side information technique for PAPR reduction in OFDM systems," in the proceedings of the International Symposium on Communications and Information Technologies (ISCIT), pp. 104 – 109, Oct. 2008.
- [8] J. Gao, J. Wang, and Z. Xie, "Reducing the peak to average power ration of OFDM system using particle swarm optimization," in the proceedings of the 4th International Conference on Wireless Communications, Networking and Mobile Computing (WiCOM), pp. 1 –4, Oct. 2008.
- [9] H. -L. Hung, Y.-F. Huang, C.-M. Yeh, and T.-H. Tan, "Performance of particle swarm optimization techniques on PAPR reduction for OFDM systems," in the proceedings of IEEE International Conference on Systems, Man and Cybernetics (SMC), pp. 2390 –2395, Oct. 2008.
- [10] S. Weinstein and P. Ebert, "Data transmission by frequency-division multiplexing using the discrete Fourier transform," IEEE Transactions on Communication Technology, vol. 19, pp. 628 – 634, Oct. 1971.
- [11] H. Liu and G. Li, OFDM-Based Broadband Wireless Networks. John Wiley and Sons, Inc, 2005.
- [12] W. Y. Y. Yong Soo Cho, Jaekwon Kim and C. G. Kang, MIMO-OFDM WIRELESS COMMUNICATIONS WITH MATLAB. John Wiley and Sons, Inc, 2010.
- [13] J. Tellado, Multicarrier Modulation With Low PAR Application to DSL and Wireless. Kluwer Academic, 2000.
- [14] A. G. Jeffery G. Andrews and R. Muhamed, Fundamentals of WiMAX. Pearson Education, Inc., 2007.
- [15] B. Vucetic and J. Yuan, Space-time coding. John Wiley and Sons, Inc, 2003.
- [16] T. Xuejian and L. Tao, "OFDM mobile communication principles and applications," □Posts and Telecommunications Press, 2003.
- [17] Y. Sun and Z. Xiong, "Progressive image transmission over space-time coded □OFDM-based MIMO systems with adaptive modulation," IEEE □Transactions on Mobile Computing, vol. 5, no. 8, pp. 1016–1028, Aug. 2006
- [18] A. D. S. Jayalath and C. Tellambura, "Side information in par reduced pts-ofdm □signals," in the proceedings of 14th IEEE Conference on Personal, Indoor and Mobile Radio Communications (PIMRC), vol. 1, pp. 226–230, Sept. 2003
- [19] H. Reddy and T. Duman, "Space-time coded OFDM with low PAPR," in the proceedings of IEEE Global Communications Conference (GLOBECOM), vol. 2, pp. 799 – 803 , Dec. 2003.

Asim M. Mazin received the B.Sc. degree in Electronic and Electrical Engineering from College of Industrial Technology (CIT) at Misurata, Libya. He worked as a teaching assistant at CIT from 2007-2010. Afterwards, he was the recipient of a scholarship from the Libyan Ministry of the Higher Education to pursue his M.S. degree. At present he is pursuing his Master of Science degree in Electrical Engineering at the Southern Illinois University Carbondale, Illinois, USA. His research interests include OFDM wireless communication, optimization techniques, and statistical signal processing.



Garth V. Crosby is an assistant professor in the department of Technology at Southern Illinois University Carbondale. He obtained his MS and PhD degrees from Florida International University in Computer Engineering and Electrical Engineering, respectively. His research interests include wireless sensor networks, ad hoc networks, wireless communication, and network security. He is a senior member of IEEE.

